British Journal of Applied Science & Technology
12(3): 1-15, 2016, Article no.BJAST.20658
ISSN: 2231-0843, NLM ID: 101664541

SCIENCEDOMAIN *international*
www.sciencedomain.org

Characterization of Low-cycle Fatigue Parameters

S. M. Humayun Kabir[1*] and Tae-In Yeo[2]

[1]Department of Mechanical Engineering, Chittagong University of Engineering and Technology, Chittagong-4349, Bangladesh.
[2]School of Mechanical and Automotive Engineering, University of Ulsan, P.O.Box 18 Ulsan 680-749, Republic of Korea.

Authors' contributions

This work was carried out in collaboration between both authors. Authors SMHK and TIY designed the research plan. Author SMHK performed the analysis of fatigue data and contributed to the writing of the manuscript. Both authors read and approved the final manuscript.

Article Information

DOI: 10.9734/BJAST/2016/20658
Editor(s):
(1) Elena Lanchares Sancho, Department of Mechanical Engineering, University of Zaragoza, Zaragoza, Spain.
Reviewers:
(1) Mohamed Afifi, MTI University, Egypt.
(2) M. C. Somasekhara Reddy, Jawaharlal Nehru Technological University, Anantapur, India.
Complete Peer review History: http://sciencedomain.org/review-history/11620

Original Research Article

Received 2nd August 2015
Accepted 31st August 2015
Published 29th September 2015

ABSTRACT

Aims: To characterize the fatigue parameters of some stainless steels at a wide range of temperatures, and also to evaluate the influence of temperature on their mechanical properties.
Methodology: Two ferritic stainless steels and one austenitic stainless steel were tested. Tensile tests under Isothermal condition are performed at room temperature and at elevated temperatures with the interval of 100ºC. Isothermal total strain-controlled fully-reversed low-cycle fatigue tests are performed at different total strain amplitudes ranging from 0.3% to 0.7% at different temperatures with a constant strain rate of 2×10^{-3} /s. The effect of temperature on elastic modulus, 0.2% yield strength, and ultimate tensile strength is demonstrated graphically. And, variation of reversals to failure with total strain amplitudes and temperatures are analyzed. Materials' constants concerning tensile and low-cycle fatigue behavior are calculated. A fatigue parameter under anisothermal condition is also assessed.
Results: The austenitic steel shows higher strength under monotonic tensile loading and lower fatigue strength under total strain-controlled fully-reversed low-cycle fatigue tests compare to others. Material strength decreases with increasing temperature. For a given total strain amplitude at low-cycle fatigue condition, when the temperature increases from room temperature to moderate

**Corresponding author: E-mail: dalimuou@yahoo.com;*

elevated temperatures, fatigue lives are higher compared to that of room temperature, and then fatigue life decreases with the further increased temperature. And, fatigue life is reduced significantly with the increasing strain amplitude for all materials considered. The fatigue parameter under anisothermal condition is found realistic from the viewpoint of safety in design.

Conclusion: Fatigue properties of materials are essential in the design and practice of mechanical structures and components subjected to cyclic loading at wide range of operating temperatures. This research contains useful monotonic and fatigue parameters which would be advantageous for the application in design and practice.

Keywords: Stainless steel; strain-controlled low-cycle fatigue; mechanical properties; fatigue parameters.

NOMENCLATURES

$\Delta\varepsilon_t / 2$	*: Total strain amplitude*
$W(T)$	*: Temperature-dependent tensile toughness*
$E(T)$	*: Temperature-dependent modulus of elasticity*
$2N_f$	*: Reversals to failure*
M, n, M_n, n_n	*: Material constants*

1. INTRODUCTION

Testing and analysis are both key parts of fatigue design. Fatigue tests are carried out to meet a set of objectives, for example; obtaining information on the cyclic response of engineering components, obtaining information regarding the behavior of a component under service loadings, and so on [1]. To understand the fatigue behavior of engineering materials completely and to perform structural integrity, several monotonic and cyclic material properties are needed. Realization of fatigue behavior and material properties derived from fatigue testing can prevent catastrophic failure of engineering structures. But, the uses of fatigue models into design and structural integrity assessment of engineering components encounter the difficulties to find references about the material properties obtained by experimental data. Therefore, characterization of fatigue mechanism and unveiling the fatigue parameters obtained from strain-controlled low-cycle fatigue tests are important steps regarding fatigue life studies. Based on the aforementioned fact, monotonic and strain-controlled low-cycle fatigue tests results of some selected ferritic and austenitic stainless steels are used as the basis of this study. These steels are developed for the use in exhaust manifold system of automobiles.

For the improvement of the efficiency of automobile engines and to reduce their weight, the use of conventional stainless steel sheets and pipes for exhaust manifolds has been increased to replace cast iron, the traditional material for this application [2]. Even though austenitic stainless steel has better strength at elevated temperatures than ferritic stainless steel, use of ferritic stainless steel has also been increased now-a-days in many high temperature structures due to its excellent corrosion resistance, moderate thermal fatigue resistance, and low prices [3]. Therefore, both ferritic and austenitic stainless steel have been used in this study to analyze the cyclic behaviors under isothermal condition at elevated temperature along with room temperature which are essential elements of reliability assessment of such structural elements. Three stainless steels, two 400-series ferritic stainless steels and one 300-series austenitic stainless steel, have been subjected to tensile and low-cycle fatigue tests.

The paper is organized as follows. Section 2 describes materials and experimental procedure. Section 3 illustrates tensile properties of materials in brief. Section 4 describes isothermal low cycle fatigue results under symmetric cyclic straining. Section 5 characterizes fatigue parameter under anisothermal condition. And finally the closing remarks are presented in section 6.

2. MATERIALS AND EXPERIMENTAL PROCEDURE

Nominal chemical compositions of as-received materials are shown in Table 1. SS300-A is a chromium-nickel austenitic stainless steel with a moderate carbon content which can be able to suppress the formation of chromium carbides during service exposure. And the ferritic stainless steels, designated here as SS400-B and SS400-

C, adopted in this study contains lower chromium-nickel and carbon than the austenitic steel.

The materials were rolled from the plate of 80 mm thickness to the plate of 20 mm, and then machined to a cylindrical bar for making specimens according to the relevant standards to perform the tensile and low-cycle fatigue tests. The specimens used in this study are fabricated with the required surface preparation in accordance with ASTM Standard E606-92 [4]. The shapes and dimensions of polished specimens used in tensile and low cycle fatigue test under strain-controlled condition are shown in Fig. 1. A closed-loop servo-hydraulic test system with 10-ton capacity manufactured by MTS Systems Corporation is used to conduct tensile and low-cycle fatigue tests. A high temperature extensometer is used during high-temperature testing which has a gage length of 12 mm, and can measure up to 20% strain. To create a high-temperature environment, the specimen is heated using induction heating method where the measurement and control of temperature is accomplished by thermocouples. Thermocouple is spot-welded on the middle of specimen to measure the temperature accurately. The experimental procedure at high-temperature consists of heating the specimen from room temperature to the testing temperature and holding at this temperature for 30 minutes before starting the test.

Tensile tests are performed at room temperature (RT) and at elevated temperatures with the interval of 100ºC. The tensile tests are carried out at a constant cross-head speed of 4.80 mm/min. In high temperature test, the signal from linear variable differential transducer (LVDT) is used to control the cross-head speed, while extensometer is used to measure the strain of the specimen. The specimen temperature is made as uniform as possible by locating the induction coil on optimal locations with optimal number of turns which is found by several pre-experiments. In this measurement, the cross-head speed of 4.80 mm/min corresponds to apparent strain rate of 2×10^{-3}/s.

Table 1. Chemical composition of stainless steels (wt%)

Materials	C	Si	P	S	Cr	Mn	Mo	Nb	Ni
SS400-B	0.015	1.00	0.04	0.03	15.00	1.00	1.65	0.5	-
SS400-C	0.025	1.00	0.04	0.03	17.00	1.00	1.12	-	-
SS300-A	0.030	1.00	0.045	0.03	19.00	2.00	-	-	11.00

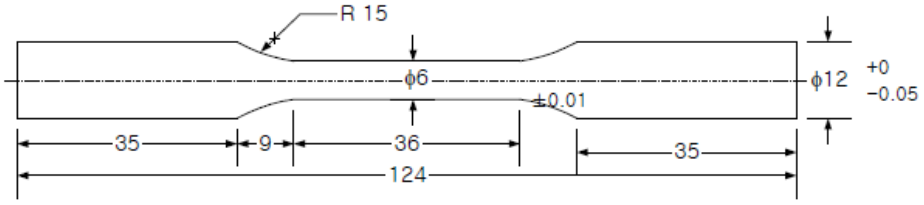

(a)

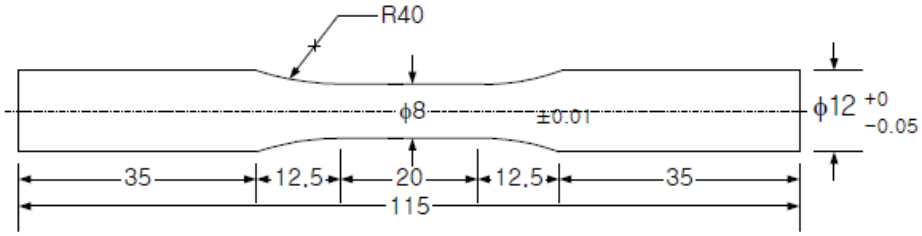

(b)

Fig. 1. Testing specimens (a) tensile and (b) Low-cycle fatigue specimen (dimensions are in mm)

Isothermal low-cycle fatigue tests are carried out under fully-reversed total strain control applying a triangular waveform with a constant strain rate of 2×10^{-3}/s. The low-cycle fatigue test are performed at different total strain amplitude ranging from $\Delta\varepsilon/2$ = 0.3% to $\Delta\varepsilon/2$ = 0.7% at different temperatures. A 10% drop in the maximum load is defined as fatigue life. The displacement, load and strain signals are measured at each cycle.

3. TENSILE TEST RESULTS

Tensile tests were carried out at room temperature and at different elevated temperatures under isothermal conditions. Figs. 2-4 demonstrate the tensile curves for different materials adopted in this study which indicate that tensile stresses under monotonic conditions decrease as temperature increases for all the materials considered. It is to be mentioned that Figs. 2-4 are generated smoothly for cleanliness where serrated flow are not visible, but the serrations occur during tensile tests for each material. The effect of temperature on elastic modulus, 0.2% yield strength, and ultimate tensile strength is shown in Figs. 5-7. The results show that there seems to be no significant effect of temperature on elastic modulus up to the temperature 300ºC and thereafter elastic modulus decreases with increasing temperature for the ferritic stainless steels, whereas in case of austenitic steel elastic modulus varies in random manner as temperature increases. Figs. 5-7 show that the austenitic stainless steel shows higher strength than the ferritic stainless steels considered at all temperatures. When the influence of temperature on material strengths, yield strength and ultimate tensile strength, are examined, material strength decreases with increasing temperature. There exists a temperature region of 200ºC - 500ºC in general for testing stainless steels considered where the strengths are retarded or slightly decreased compared with other temperature regime. This phenomenon can be attributed to the dynamic strain ageing [5]. This anomalous dependence of tensile properties in the dynamic strain ageing regime has also been observed in other classes of steel in recent studies [6,7]. The occurrence of dynamic strain ageing during plastic deformation is an important phenomenon in metallic materials [5,8-10]. The underlying physical mechanisms have been the object of many academic studies [11,12]. Dynamic strain ageing which is attributed to the interaction of solute atoms with moving dislocations, is generally observed when the deformation temperature is high enough to permit short range diffusion of solute atoms to dislocation cores. However, complete evidences of dynamic strain ageing of SS400-B can be found elsewhere [12].

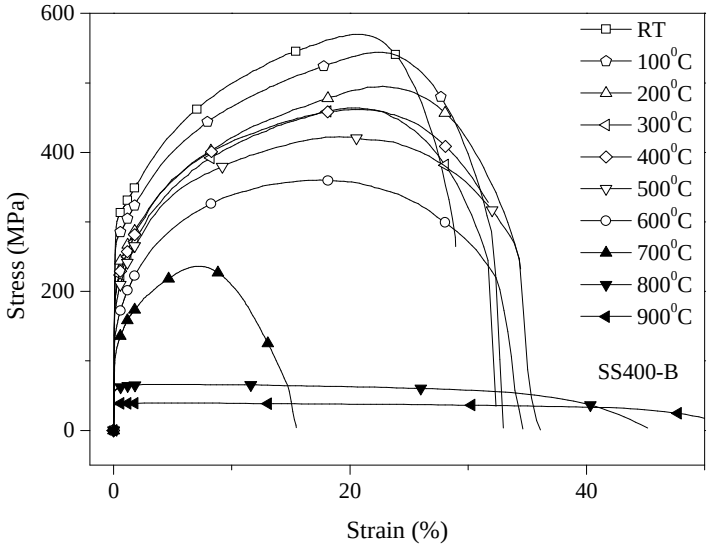

Fig. 2. Tensile curves of SS400-B at various temperatures

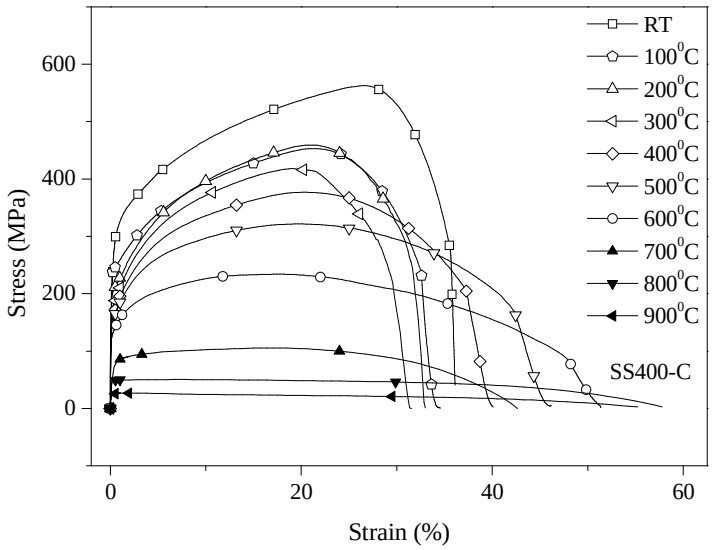

Fig. 3. Tensile curves of SS400-C at various temperatures

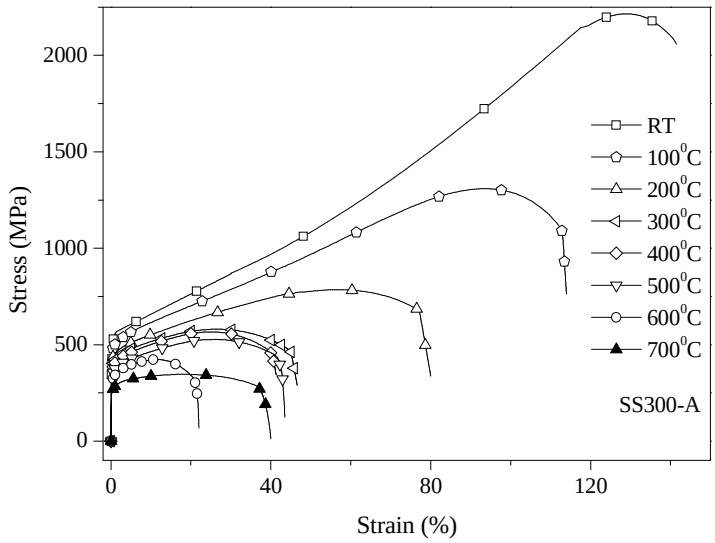

Fig. 4. Tensile curves of SS300-A at various temperatures

4. ISOTHERMAL LOW CYCLE FATIGUE RESULTS UNDER SYMMETRIC CYCLIC STRAINING

During services as many automotive engine components, for example exhaust manifold systems, are exposed to high temperature, low cycle fatigue data for describing material inelastic responses under high temperature cyclic loading conditions are necessary. The total strain-controlled fully-reversed cyclic tests were conducted at several temperature levels ranging from room temperature to 800ºC. These temperatures would cover the whole temperature range which may come into questions concerning the temperature variation experienced by exhaust manifold operation. The tests were performed at different constant strain amplitude, namely, 0.3%, 0.4%, 0.5%, 0.6% and 0.7%. However, in case of SS400-B, barreling phenomenon is observed above 700ºC in the test which can be ascribed to several constraints including the positional variation or gradient in the cyclic stress-strain field caused by geometry, temperature, or material variations during low cycle fatigue test. The strain amplitudes and

stress amplitudes are determined at stabilized loop of each specimen. Figs. 8-10 show the variation of total strain amplitudes with the number of reversals to failure for the stainless steels at various temperatures. In Figs. 8-10, the lines represent the best-fit curves of linear relationship in a double logarithmic plot for the data set at different temperatures.

From total strain amplitude - reversals to failure curves of Figs. 8-10, it can be seen that SS400-C exhibit more scatter data than that of SS400-B and SS300-A. And SS300-A clearly has inferior strength in the low cycle fatigue regime. It is also seen that fatigue life is reduced significantly with the increasing strain amplitude. For a given moderate total strain amplitude, in case of SS400-B, when the temperature increases from room temperature to 200ºC and 300ºC, fatigue lives are higher, and then fatigue life decreases with the further increased temperature above 300ºC compared to that of room temperature. But for all strain amplitude, in case of the austenitic steel SS300-A, the total strain amplitude-life endures for longer up to the temperature level of 400ºC as the temperature is elevated, whereas fatigue life decreases notably when temperature increases further above 400ºC. In case of SS400-C, the effect of temperature on life is somewhat complex.

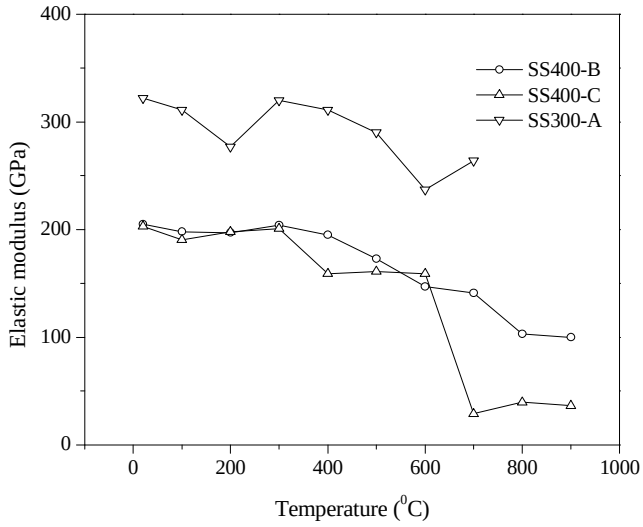

Fig. 5. Temperature dependent mechanical properties (Elastic Modulus)

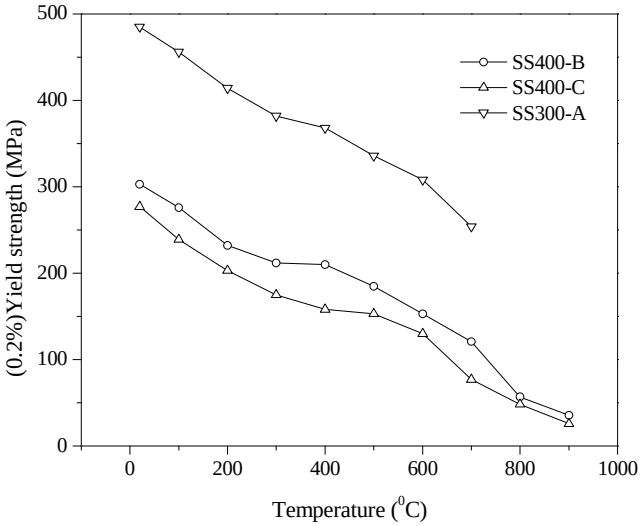

Fig. 6. Temperature dependent mechanical properties (Yield Strength)

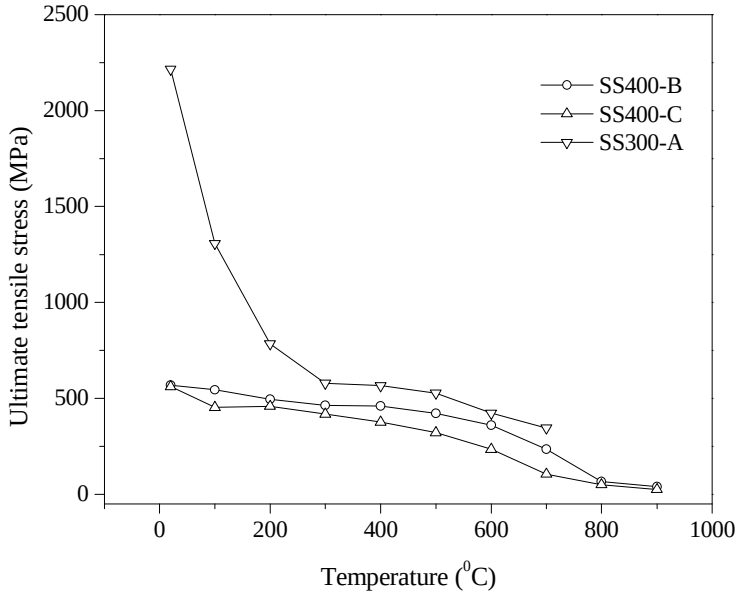

Fig. 7. Temperature dependent mechanical properties (Ultimate Tensile Stress)

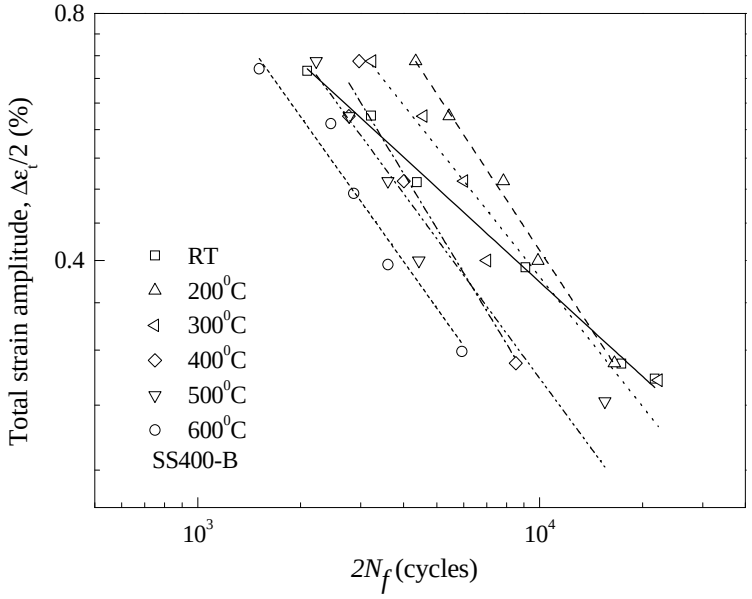

Fig. 8. Low-cycle fatigue lives of SS400-B at different temperatures

Several researchers have also reported the strong influence of temperature on low cycle fatigue life of various stainless steels [13-18]. At intermediate temperatures, usually the time dependent processes have no substantial effects, yet the drastic reduction in low cycle fatigue life is also observed with increasing temperature and decreased strain rate in alloys such as Nimonic PE 16 superalloy [19], Haynese 188 superalloy [17], Hastealloy [14] and Duplex stainless steel [20]. The reduction of fatigue life with respect to temperature of SS400-B is attributed to dynamic strain ageing [12].

SS300-A shows somewhat differences in reduction of fatigue life with respect to temperatures compared to that of SS400-B. Although serrations appear in monotonic stress-strain curves, SS300-A austenitic steel shows no enhanced stress response and experiences

cyclic softening (Fig. 11) at all elevated temperatures as opposed to the pronounced hardening of SS400-B (Fig. 12). And SS300-A shows no remarkable differences in life for the temperature range of 200ºC – 400ºC (Fig. 10). Fig. 11 depicts that cyclic softening behavior is observed throughout the whole life time. The cyclic softening continues to the macro-crack initiation point which results steep decrease of peak stress. The higher the total strain amplitude, the lower the fatigue strength. Cyclic softening was also experimentally observed for the austenite steel of the type 316L [21]. For the present material, it is shown that, during cyclic softening, the decrease of the stress amplitude with the logarithm of loading cycles is close to linear most of the case, i.e. the softening rate decreases with the inverse of the number of loading cycles.

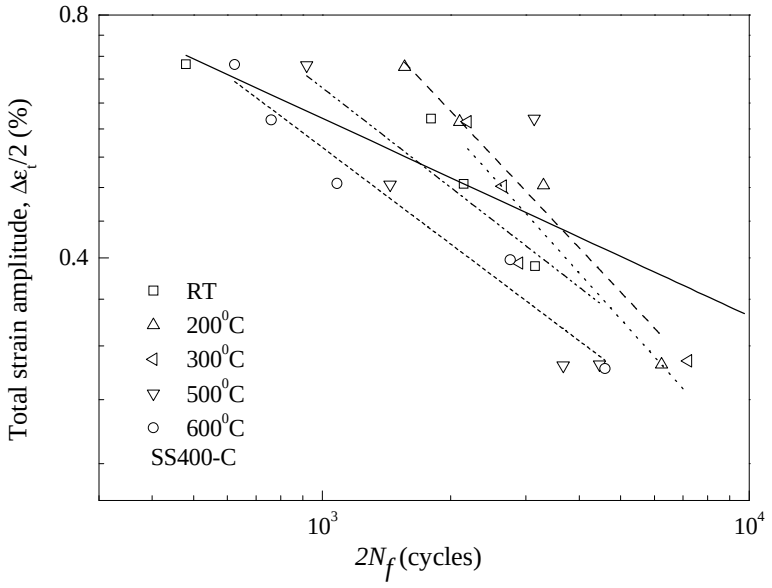

Fig. 9. Low-cycle fatigue lives of SS400-C at different temperatures

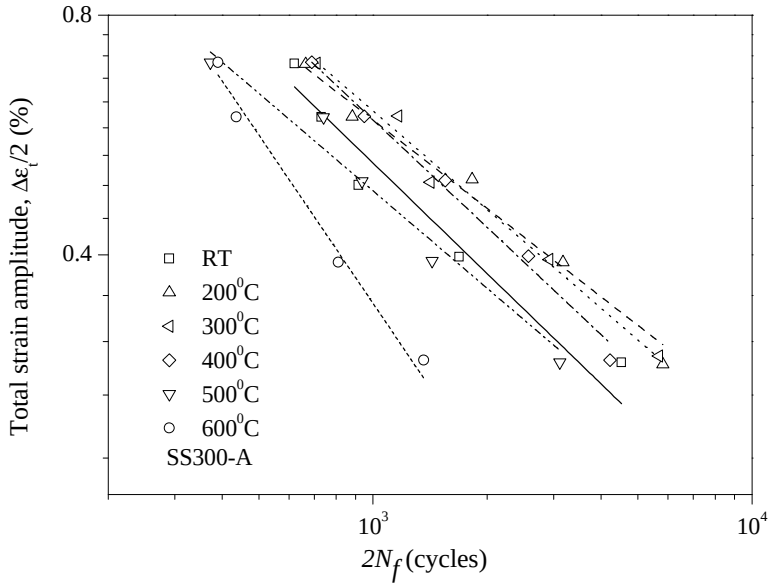

Fig. 10. Low-cycle fatigue lives of SS300-A at different temperatures

However, the fatigue life curve can be represented by the following Eq. (1) of total strain amplitude- reversal to failure,

$$\frac{\Delta\varepsilon_t}{2} = M(2N_f)^n \quad (1)$$

The double logarithmic plots of total strain amplitude ($\Delta\varepsilon_t/2$) and reversals to failure ($2N_f$) provide reasonable linear relationship for each temperature. The corresponding material constants *M* and *n* are listed in Table 2. It is worthy to note that the low-cycle fatigue properties for obtaining cyclic stress-strain curves of the materials at room temperature can be found elsewhere [12,22].

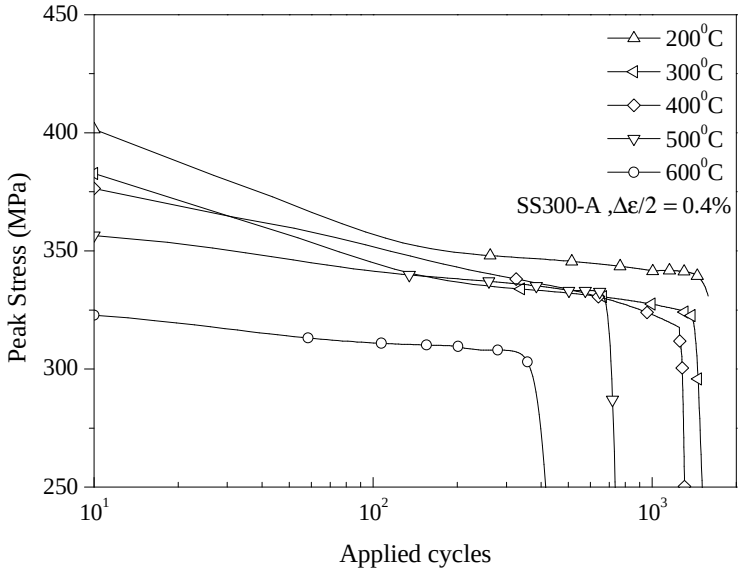

Fig. 11. Typical influence of temperatures on evolution of peak stress of SS300-A

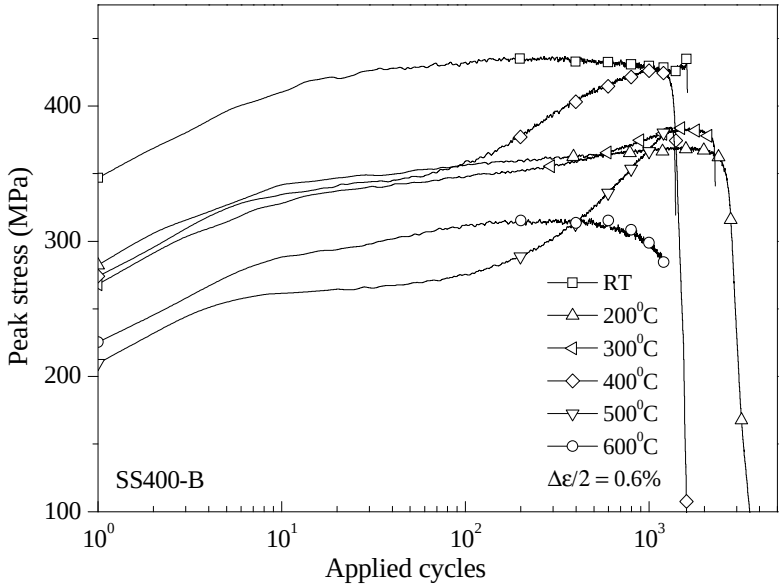

Fig. 12. Typical influence of temperatures on evolution of peak stress of SS400-B

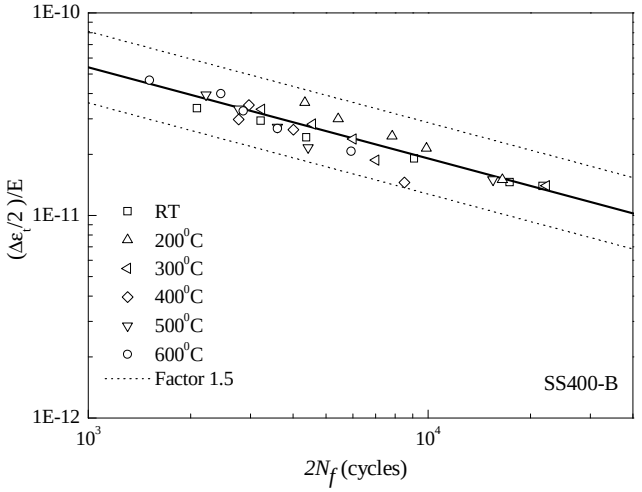

(a)

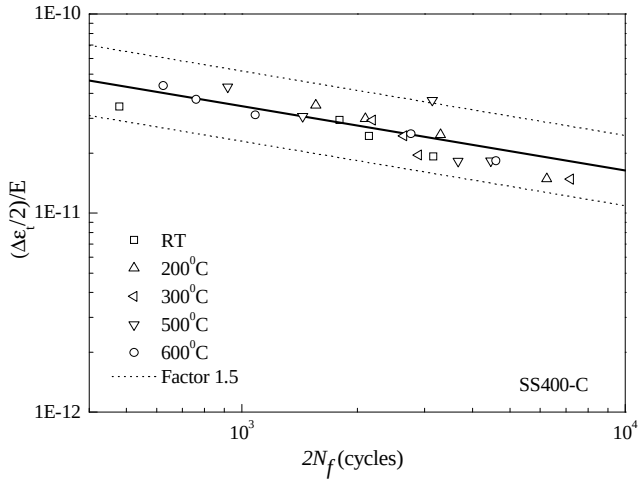

(b)

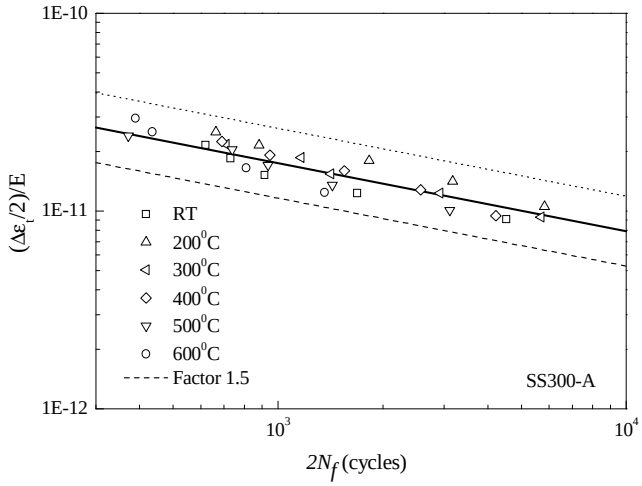

(c)

Fig. 13. Correlation between damage parameter $(\Delta\varepsilon_t/2)/E(T)$ and reversals to failure for (a) SS400-B, (b) SS400-C, and (c) SS300-A

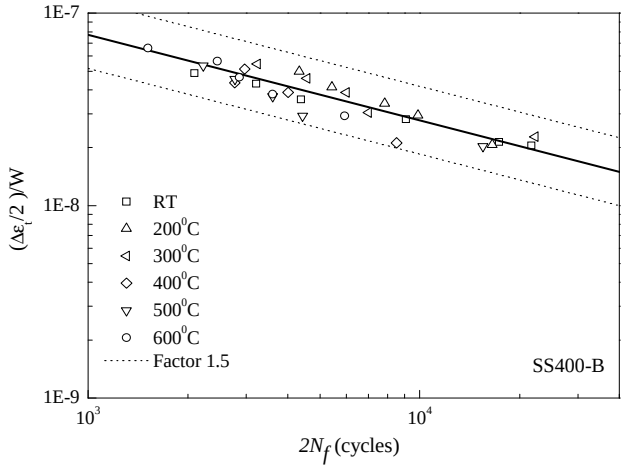

(a)

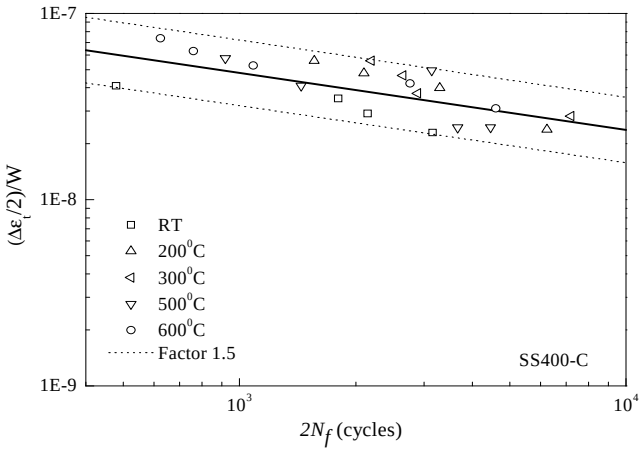

(b)

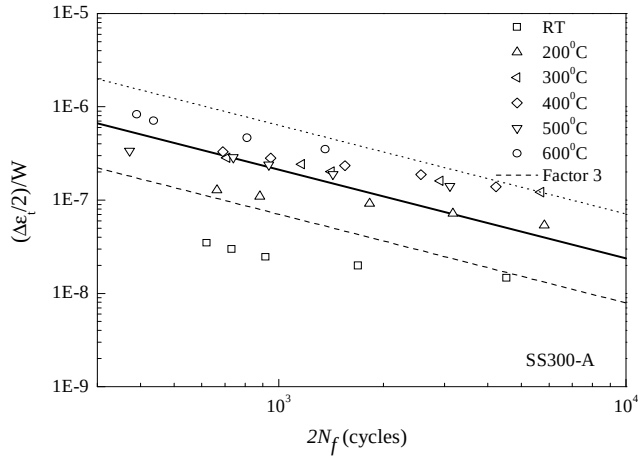

(c)

Fig. 14. Correlation between damage parameter $(\Delta\varepsilon_t/2)/W(T)$ and reversals to failure for (a) SS400-B, (b) SS400-C, and (c) SS300-A

5. THERMO-MECHANICAL FATIGUE PARAMETERS

Stainless steels considered in this research have been analyzed at a wide range of temperatures under isothermal condition. Life prediction models for isothermal condition have been modified to predict life under anisothermal condition by introducing suitable factors to compensate the influence of temperature on fatigue life by various researchers [8,23-25]. It is because; thermal fatigue test facilities are complicated and time-consuming. Moreover, complex models with high number of parameters need difficult identification procedure and many fatigue tests. From the point of view for a fast practical industrial application, empirical formulation with the following features is preferred [25]; moderate number of parameters, parameters are readily obtainable from simple monotonic and cyclic test, and good life prediction capability. Inspiring from above mentioned facts, Eq. (1) is modified in the following manner to reflect temperature effect on fatigue life,

$$\left(\Delta\varepsilon_t/2\right)/X(T) = M_n(2N_f)^{n_n} \quad (2)$$

where, X(T) is a temperature dependent material property which is incorporated in the damage parameter of Eq. (1) to compensate the influence of temperature on fatigue life. M_n and n_n are material constants. The objective of each of procedure of fatigue life prediction is to collapse all fatigue data (at whole range of temperature) onto/around a single curve. The fatigue lives are plotted against the modified damage parameter $\left(\Delta\varepsilon_t/2\right)/X(T)$ using Eq. (2) in Figs. 13-14 for whole range of temperatures. Temperature dependent material property $X(T)$ is modulus of elasticity E(T) and tensile toughness W(T) in Figs. 13 and 14 respectively. Results shows that fatigue life data at different temperatures are fairly collapsed onto/around a single line except Fig. 14(c). The solid line is a least square fitting curve and material constants M_n and n_n are extracted from regression analysis which are provided in Tables 3-4. The performance of fatigue parameter $\left(\Delta\varepsilon_t/2\right)/W(T)$ appears to poor with most of data points disperse from the solid line (Fig. 14). Fig. 13 depicts that the scatter band is of ±1.5 and the damage parameter $\left(\Delta\varepsilon_t/2\right)/E(T)$ offered by Eq. (2) is found to yield good correlation for all materials considered.

For the evaluation of fatigue damage parameter $\left(\Delta\varepsilon_t/2\right)/E(T)$, reversals to failure are predicted using material constants of Table 3. The predicted reversals to failure are compared with experimental reversals to failure through Figs. 15(a)-(c) in which diagonal line represents the perfect correlation line. In general, reasonably good correlations are observed between predicted and experimental lives for materials considered.

Table 2. Material constants under strain-controlled Low-cycle fatigue tests

Temp	SS400-B		SS400-C		SS300-A	
	M	n	M	n	M	n
RT	0.1275	-0.3824	0.0324	-0.2451	0.1258	-0.4608
200ºC	1.4236	-0.6347	0.4389	-0.5630	0.0756	-0.3691
300ºC	0.4843	-0.5256	0.5112	-0.5900	0.1042	-0.4166
400ºC	1.5625	-0.6900	-	-	0.1307	-0.4483
500ºC	0.5272	-0.5658	0.1110	-0.4108	0.0797	-0.4064
600ºC	0.5138	-0.5857	0.0861	-0.3988	0.4427	-0.7017

Table 3. Normalized material constants when X = E(T)

SS400-B		SS400-C		SS300-A	
M_n	n_n	M_n	n_n	M_n	n_n
1.2123E-09	-4.5041E-01	3.2503E-10	-3.2459E-01	1.8741E-10	-3.4357E-01

Table 4. Normalized material constants when X = W(T)

SS400-B		SS400-C		SS300-A	
M_n	n_n	M_n	n_n	M_n	n_n
1.6665E-06	-4.4449E-01	4.0000E-07	-3.0689E-01	1.5000E-04	-9.5022E-01

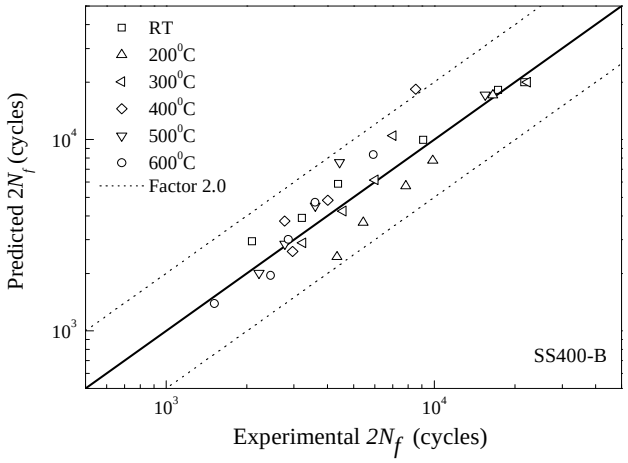

(a)

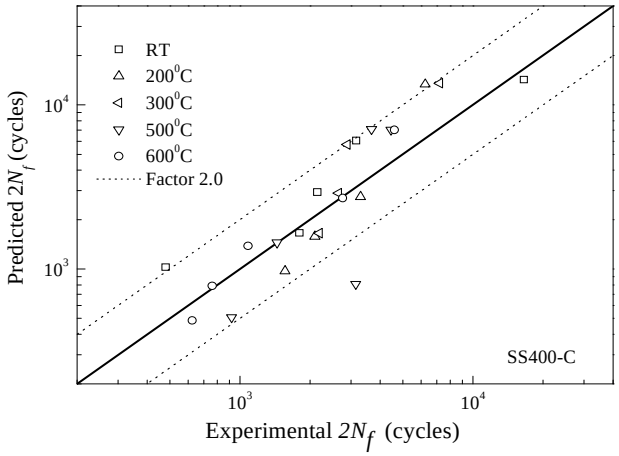

(b)

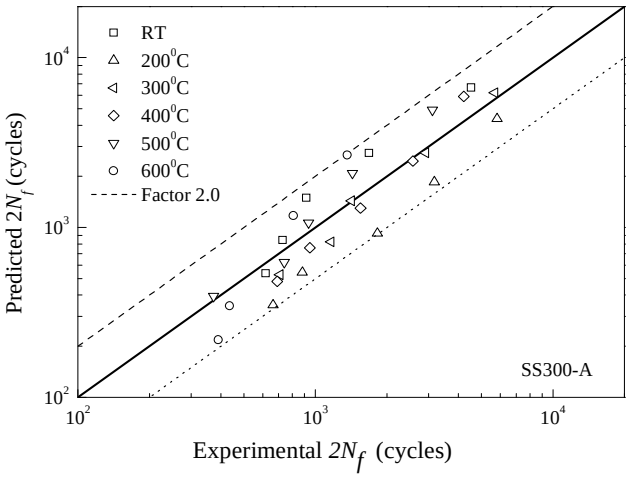

(c)

Fig. 15. Comparison of calculated and experimental reversals to failure using damage parameter $(\Delta\varepsilon_t/2)/E(T)$ for (a) SS400-B, (b) SS400-C, and (c) SS300-A

6. CONCLUSION

Three stainless steels, two ferritic stainless steels and one austenitic stainless steel, are studied under tensile monotonic and strain-controlled low-cycle fatigue tests at a wide range of temperatures. The obtained results are as following:

a) The austenitic steel shows higher strength under monotonic tensile loading compare to others for the whole range of temperatures tested.
b) The austenitic steel shows lower fatigue strength compare to others.
c) Softening rate decreases with the inverse of the number of loading cycles for the austenitic stainless steel considered.
d) Tests results have shown a strong influence of temperature and strain amplitude on monotonic responses as well as on low cycle fatigue responses.
e) The log-log plots of total strain amplitudes and reversals to failure provide reasonable linear relationship for each temperature.
f) Constants associated with damage parameter discussed under anisothermal condition are readily obtainable from simple monotonic and cyclic test.
g) Fatigue properties of materials are essential in the design and practice of mechanical structures and components subjected to cyclic loading at wide range of operating temperatures. Therefore, this research would be advantageous to find monotonic and fatigue parameters for the application in design and practice.

ACKNOWLEDGEMENT

The authors express their thanks to SEJONG INDUSTRIAL CO. LTD., Republic of Korea for their support in acquiring of the material data.

COMPETING INTERESTS

Authors have declared that no competing interests exist.

REFERENCES

1. Swanson SR, editor. Handbook of fatigue testing. STP 566. Philadelphia (PA): ASTM; 1974.
2. Fujita N, Ohmura K, Kikuchi M, Suzuki T, Funaki S, Hiroshige I. Effect of Nb on high-temperature properties for ferritic stainless steel. Scripta Mater. 1996;35:705-10.
3. Beddos J, Parr JG. Introduction to stainless steels. 3rd ed: ASM Intl; 1998.
4. ASTM E606. Standard practice for strain-controlled fatigue testing. Conshohocken: ASTM; 1998.
5. Cottrell AH, Bilby BA. Dislocation theory of yielding and strain ageing of iron. Proc Phys Soc A. 1949;62:49-62.
6. Meng LJ, Sun J, Xing H, Pang GW. Serrated flow behavior in AL6XN austenitic stainless steel. J Nucl Mater. 2009;394(1): 34-38.
7. Nagesha A, Goyal S, Nandagopal M, Parameswaran P, Sandhya R, Mathew MD, Mannan SK. Dynamic strain ageing in Inconel® Alloy 783 under tension and low cycle fatigue. Mater Sci Eng A. 2012;546: 34-39.
8. Hong SG, Lee SB. Influence of strain rate on tensile and LCF properties of prior cold worked 316L stainless steel in dynamic strain aging regime. In: Varvani-Farahani A, Brebbia CA, editors. Fatigue damage of materials: Experiment and analysis. Southampton: WIT Press. 2003;40.
9. McCormick PG. Theory of flow localization due to dynamic strain ageing. Acta Metall. 1988;36(12):3061-67.
10. Nandy K, Feng Q, Pollock TM. Elevated temperature deformation and dynamic strain aging in polycrystalline RuAl alloys. Intermetallics. 2003;11:1029-38.
11. Kubin LP, Estrin Y. Dynamic strain ageing and mechanical response of alloys. Journal De Physique III. 1991;1:929-43.
12. Kabir SMH, Yeo T. Evaluation of an energy-based fatigue approach considering mean stress effects. J Mech Sci Technol. 2014;28(4):1265-75.
13. Armas AF, Bettin OR, Alvarez-Armas I, Rubiolo G. Strain aging effects on the cyclic behavior of austenitic stainless steels. J Nucl Mater. 1988;155–157(2): 644-49.
14. Castelli MG, Miner RV, Robinson DN. Thermomechanical deformation behavior of a dynamic strain ageing alloy, Hastelloy X. In: Sehitoglu editor. Thermomechanical Fatigue Behavior of Materials. STP 1186. Philadelphia: ASTM; 1993.
15. Rao KBS, Valsan M, Sandhya R, Mannan SL, Rodriguez P. Dynamic strain ageing effects in low cycle fatigue. High Temp Mater Proc. 1986;7:171-77.

16. Tsuzaki K, Hori T, Maki T, Tamura Y. Dynamic strain aging during fatigue deformation in type 304 austenitic stainless steel. Mater Sci Eng A. 1983;61:247-60
17. Rao KBS, Castelli MG, Ellis JR. On the low cycle fatigue deformation of haynes 188 superalloy in the dynamic strain aging regime. Scripta Metall Mater. 1995;33: 1005-12.
18. Zauter R, Petry F, Christ H-J, Mughrabi H. Thermomechanical fatigue of the austenitic stainless steel AISI 304L. In: Sehitoglu editor. Thermomechanical fatigue behavior of materials. STP 1186. Philadelphia: ASTM; 1993.
19. Valsan M, Sastry DH, Rao KBS, Mannan SL. Effect of strain rate on high-temperature low-cycle fatigue properties of a Nimonic PE-16 superalloy. Metall Trans. 1995;25A:159-71.
20. Herenu S, Alvarez-Armas I, Armas AF. The influence of dynamic strain aging on the low cycle fatigue of duplex stainless steel. Scripta Mater. 2001;45:739-45.
21. Hong SG, Lee SB. The tensile and low-cycle fatigue behavior of cold worked 316L stainless steel: Influence of dynamic strain aging. Int J Fatigue. 2004;26:899–910.
22. Kabir SMH, Yeo T. Fatigue behavior of an austenitic steel of 300-series under non-zero mean loading. J Mech Sci Technol. 2012;26(1):63-71.
23. Shi XQ, Pang HLJ, Zhou W, Wang ZP. A modified energy-based low cycle fatigue model for eutectic solder alloy. Scripta Mater. 1999;41(3):289-96.
24. Lee KO, Hong SG, Yoon S, Lee SB. A new high temperature life correlation model austenitic and ferritic stainless steel. Int J Fatigue. 2005;27:1559-63.
25. Gocmez T, Awarke A, Pischinger S. A new low-cycle fatigue criterion for isothermal and out-of-phase thermomechanical loading. Int J Fatigue. 2010;32:769-79.

Peer-review history:
The peer review history for this paper can be accessed here:
http://sciencedomain.org/review-history/11620